JOURNAL OF CATALYSIS 50, 24–34 (1977)

# Methanol Partial Oxidation at Low Temperature

JAMES EDWARDS

*General Electric Corporation, Schenectady, New York 12345*

JOHN NICOLAIDIS

*Creole Petroleum Company, Judibana, Edo. Falcon, Venezuela*

M. B. CUTLIP AND C. O. BENNETT

*Department of Chemical Engineering, University of Connecticut, Storrs, Connecticut 06268*

Received December 31, 1976

The partial oxidation of methanol was investigated in a mixed flow reactor at atmospheric pressure. A lean methanol–air mixture was passed over a commercial iron–molybdenum oxide catalyst to obtain steady-state reaction rates at temperatures from 170 to 367°C. Transient experiments were also performed at 170°C, where the principal products were formaldehyde, water, dimethyl ether, methyl formate, and methylal. The results suggest that $OCH_3$ on the surface plays an important part in the reaction sequence.

## INTRODUCTION

The partial oxidation of methanol for formaldehyde over mixtures of iron and molybdenum oxides has been extensively studied since the early 1960's. The present work contributes further to knowledge of the kinetics of the reaction, with particular emphasis on the role of adsorbed methoxyl intermediates. The transient method (*1*) was employed in addition to steady-state rate measurements. A typical commercial catalyst was used: $Fe_2(MoO_4)_3$ plus $MoO_3$ with a total atomic ratio Mo/Fe = 3.0.

Pernicone *et al.* (*2*) have proposed that oxygen doubly bonded to Mo interacts with methanol to form

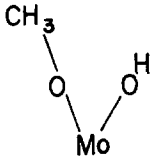


The $CH_3O$– is then dehydrogenated to adsorbed formaldehyde; the hydrogen removed combines with oxygen to form more –OH groups. They considered that the desorption of formaldehyde is the rate-determining process. However, the –OH groups also desorb slowly, and water in the gas phase is a strong inhibitor, reacting with Mo–O to form

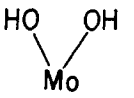


as with acid sites. This concept is supported by the observation that pyridine also poisons the catalyst surface (*3*). As formaldehyde and water desorb, the exposed Mo sites are reoxidized by mobile oxygen from the lattice. For low methanol partial pressures the rate equation of Mars and van Krevelan (*4*) may be satisfactory (*5*), but for high conversions the





ISSN 0021-9517

effect of water must be included, possibly as proposed by Evmenenko and Gorokhovatskii (*6*);

$$r = k \frac{(\mathrm{MeOH})}{1 + b_1(\mathrm{MeOH}) + b_3(\mathrm{H_2O})} \cdot \frac{(\mathrm{O_2})}{1 + b_2(\mathrm{O_2})} \quad (1)$$

The presence of iron in the catalyst appears to facilitate electron transfer so that $Mo^{6+}$ is not irreversibly reduced to $Mo^{4+}$ during reaction (with $O_2$ present) as it is with pure $MoO_3$ (*7*). Over this catalyst formaldehyde was obtained at first, but as the Mo was reduced the product became CO; no $CO_2$ was formed.

## EXPERIMENTAL DETAILS

The reactor system is shown in Fig. 1; it was made of stainless steel, with the exception of the glass methanol saturator. The reactor, recycle pump, and sampling valve were contained in a valve oven kept at 146°C to prevent the polymerization of formaldehyde and condensation of the reaction mixture. The reactor temperature was separately controlled. A recycle ratio of at least 20/1 was maintained by a metal bellows pump so that the reactor/recycle loop was completely mixed at all times. A bypass line around the saturator permitted adjustment of the methanol concentration in the feed also containing $N_2/O_2$ in the molar ratio 4/1.

The reactor itself was made from a 304 stainless-steel cylinder 69.8 mm in diameter and 50.8 mm long, as shown in Fig. 2. The catalyst is held in seven holes in the block. Removable screens hold the particles in place. The two end closures are sealed by standard vacuum metal gaskets of aluminum. Isothermal operation is assured by the small conversion per pass through the reactor, by the massive metal block, and by the high surface-to-volume ratio of the catalyst spaces. The reactor was heated above 146°C (the oven temperature) by six cartridge heaters placed in the walls as shown in Fig. 2.

Blank runs were made at typical operating temperatures with no catalyst in place. Copper gaskets were found to cause some conversion of methanol to $CO_2$, so they were replaced by aluminum gaskets; with these, there was no conversion in the recycle system. During the measurements the catalyst bed occupied about 25 ml in the reactor. The sum of the clearance and displacement volumes of the bellows pump was about 3 ml, so that the total volume

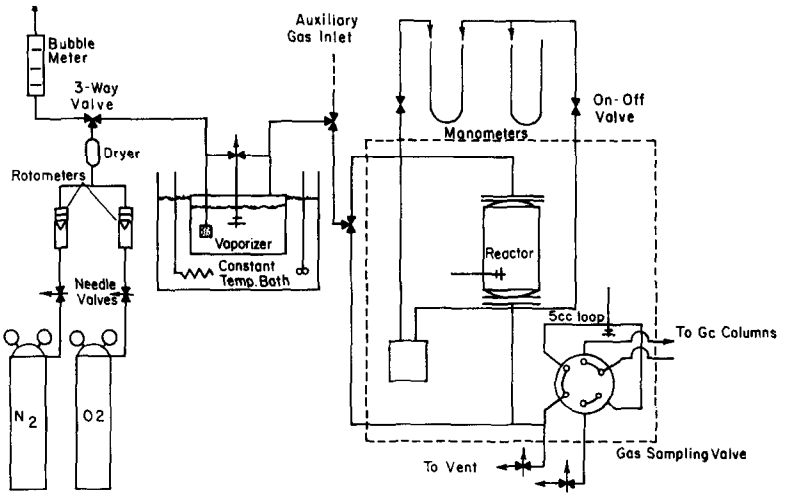


FIG. 1. Methanol oxidation process flow sheet.

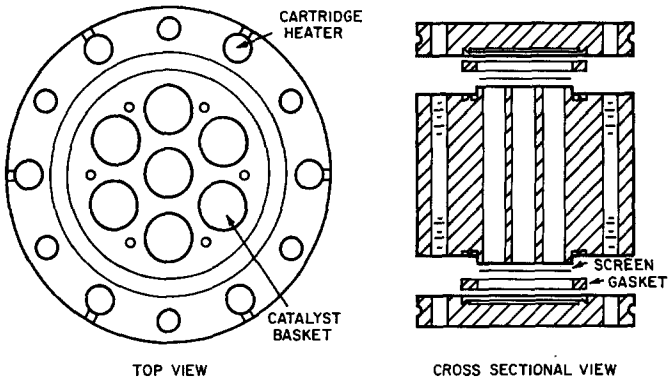


FIG. 2. Reactor schematic.

in the recycle system outside of the catalyst beds was less than 5 ml. The pressure drop across the reactor when operating full of catalyst was 16 in. of water, corresponding to a recycle flow rate of 5900 ml/min. Net flow rates through the system were typically less than 300 ml/min, so that the recycle system behaved as a continuous flow stirred-tank reactor. For some high-temperature runs a higher feed flow was required; in such cases the rates were calculated based on a plug-flow reactor with recycle.

A 5-ml sample was sent to the chromatographic column system shown in Fig. 3. A typical chromatogram obtained with a carrier gas flow of 50 ml/min is shown in Fig. 4. The light gases, $O_2$, $N_2$, and CO, passed quickly through the Poropak columns at 170°C and into the molecular sieve column. The switching valve was then turned so that the other gases eluted as shown while the light gases were trapped in the molecular sieve column. Afterwards, the oven was cooled to 60°C and the switching valve was returned to its original position to elute the light gases. The entire analysis took about 1 h. Relative response factors based on methanol were obtained by calibration with known mixtures and pure species and are given in Table 1.

The reactor was filled with a commercially available iron–molybdenum oxide catalyst made by Harshaw and supplied by the Lummus Company. This catalyst was composed of two phases, ferric molybdate and molybdenum trioxide, with an atomic molybdenum to iron ratio of 3.0. This unsupported catalyst, which came as pellets, was crushed and separated into 0.25- to 0.59-mm sizes. Then 24.18 g of the catalyst were poured into the reactor and activated by passing 75 ml/min of an

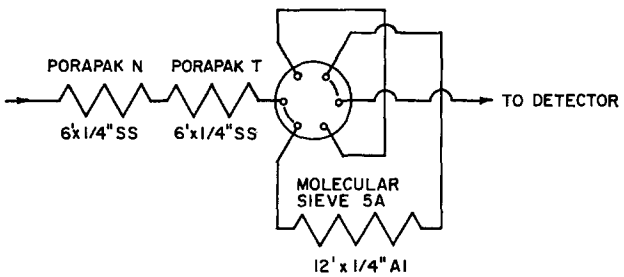


FIG. 3. Column system for gas chromatography.

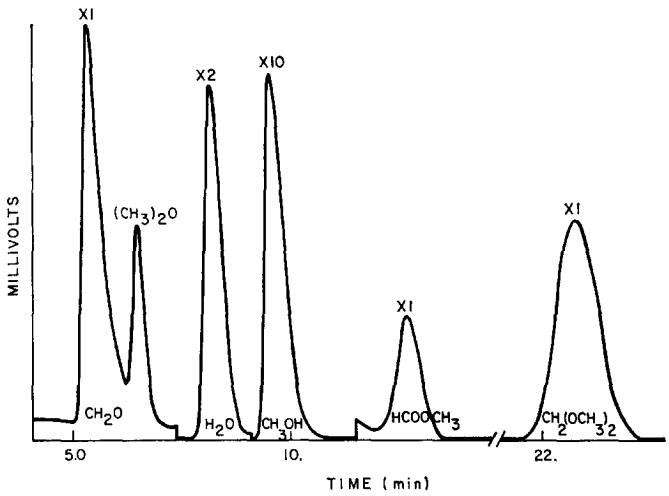


FIG. 4. Chromatogram of reaction products: column temperature, 170°C.

80% $N_2$–20% $O_2$ gas mixture over the catalyst for nearly 15 h at a temperature of 320°C. The specific surface area after activation was measured with a Perkin-Elmer sorptometer and found to be 4.6 $m^2/g$. The density of the pellets was 2.15 g/ml and the porosity of the catalyst bed was calculated as 0.5. This catalyst has also been characterized with X-ray diffraction by Aruanno and Wanke (*9*).

## RESULTS

Both the steady-state and transient rate measurements indicated that in addition to production of formaldehyde and carbon monoxide at all temperatures, appreciable amounts of dimethyl ether, methyl formate, and methylal were formed at the lowest experimental temperature. The observed reactions were the following.

$r_1$ $CH_3OH + \frac{1}{2}O_2 \rightarrow CH_2O + H_2O$

$r_2$ $2CH_3OH \rightarrow (CH_3)_2O + H_2O$

$r_3$ $2CH_3OH + O_2 \rightarrow HCOOCH_3 + 2H_2O$

$r_4$ $3CH_3OH + \frac{1}{2}O_2 \rightarrow CH_2(OCH_3)_2 + 2H_2O$

$r_5$ $CH_2O + \frac{1}{2}O_2 \rightarrow CO + H_2O$

These individual rates were calculated by the mathematical treatment which follows.

A network of $R$ simultaneous reactions involving $N$ chemical species can be described by the following equation:

$$\sum_{j=1}^{N} \alpha_{ij} A_j = 0; \quad i = 1, 2, \ldots, R \qquad (2)$$

The stoichiometric coefficient $\alpha_{ij}$ is positive for products and negative for reactants.

A steady-state material balance on a mixed flow reactor for the $j$th species of a particular network can be expressed as:

$$F_0 y_{fj} + W \sum_{i=1}^{R} \alpha_{ij} r_i = F_p y_j. \qquad (3)$$

The material balance can also be summed

TABLE 1

Response Factor Relative to Methanol

| Species | Mean response factor | Standard deviation |
|---|---|---|
| $O_2$ | 1.08 | 0.04 |
| $N_2$ | 1.01 | 0.03 |
| $H_2O$ | 1.74 | 0.04 |
| $CH_2O$ | 1.09 | 0.02 |
| $(CH_3)_2O$ | 0.64 | 0.04 |
| $HCOOCH_3$ | 0.76 | 0.02 |
| $CH_2(OCH_3)_2$ | 0.57 | 0.02 |

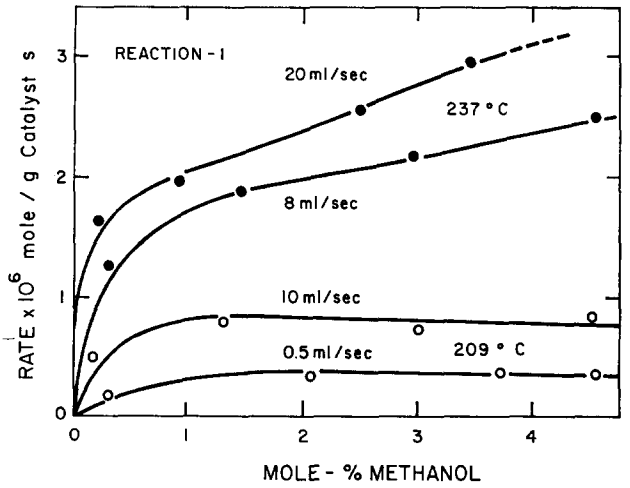


FIG. 5. Steady-state rate vs mol % methanol: low temperature range.

over all of the $N$ species:

$$F_0 + W \sum_{i=1}^{R} \bar{\alpha}_i r_i = F_p, \qquad (4)$$

where $\bar{\alpha}_i = \sum^{N}_{j=1} \alpha_{ij}$ for convenience. Then Eq. (4) can be used to eliminate $F_p$ in Eq. (3), and thus account for molar changes occurring in the reaction network:

$$\sum_{i=1}^{R} (\bar{\alpha}_i y_j - \alpha_{ij}) r_i = \frac{F_0}{W} (y_{fj} - y_j). \qquad (5)$$

In the general case all five $r_i$ values can be determined from the measurement of $F_0/W$ and the mole fraction $y_j$ of the five carbon-containing products. These values are substituted into Eqs. (5) and the $r_i$ values are found by their simultaneous solution. In this work $y_{fj}$ was zero for each of these products. At 173°C $r_5$ was negligible and all the other products were formed. At 209°C and higher, only $CH_2O$ and CO were detected in any appreciable quantity.

TABLE 2

Reaction Rates ($\times 10^8$ mol/g·sec) at 173°C

| Flow of $N_2$–$O_2$ (ml/min) | $r_1$ | $r_2$ | $r_3$ | $r_4$ |
|---|---|---|---|---|
| 10 | 6.7 | 0.67 | 4.4 | 0.67 |
| 50 | 18. | 1.7 | 3.4 | 13.0 |
| 150 | 20. | 5.0 | 2.5 | 30 |

Steady-state results for 209 and 237°C are given in Fig. 5. Two feed rates were used at each temperature; a high flow rate corresponds to a short residence time and a low conversion. By using various concentrations of methanol in the reactor feed, the two lines shown were obtained. The rates at high conversion are lower because of inhibition by the reaction products. For 173°C the calculated rates are given in Table 2.

Data at other temperatures for reactions 1 and 5 are given in Figs. 6 and 7. Figure 8 is an Arrhenius plot for the formaldehyde production at 1.25 mol % methanol. The measurements at the four lowest temperatures fall on a straight line corresponding to an activation energy of 19.5 kcal/mol (4.18 kJ = 1 kcal). The rates at the two highest temperatures fall below the extension of the straight line. The existence of this straight line is probably the best proof of the absence of heat and mass transfer falsification in this temperature range. Above 280°C the effectiveness factor is the ratio of the rate

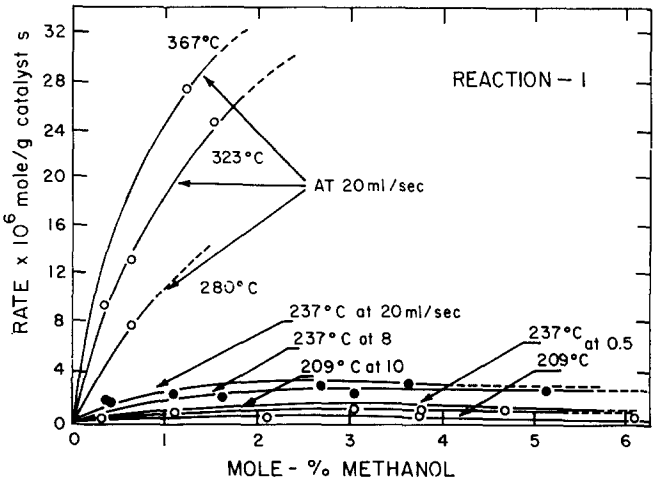


FIG. 6. Steady-state rate vs mol % methanol.

measured to that given by the extension of the straight line.

Table 3 shows typical rates and activation energies taken from the other studies from which such quantities could be obtained under conditions comparable to those used in the present work. The activation energy reported here is the highest in the table, furnishing further evidence of the absence of transport limitations in the measured rates. Above 280°C the slope on the Arrhenius plot even falls below one-half the activation energy so that interphase temperature and concentration gradients are indicated.

It may be of some interest to calculate the isothermal effectiveness factor according to the standard procedures given, for example, by Carberry (*10*) for a first-order reaction for a spherical particle. The result depends on the assumption of a tortuosity [$\tau = 3.0$ was chosen, following Satterfield (*11*) for a catalyst of similar specific surface] and on the calculation of a mean pore diameter by the approximate equation (*11*):

$$r_e = \frac{2\theta}{S_g \rho_p}. \qquad (5a)$$

At 280°C the necessary parameters and results are given in Table 4, leading to $\eta = 0.72$. Considering the approximate nature of the calculation, it is reasonable to suppose that the rate at 280°C is in a region just about to be influenced by mass transfer effects, as shown in Fig. 8. The value of $\beta$ indicates an isothermal pellet.

It is even more difficult to make an accurate estimation of the interphase temperature difference, for the relation between the fluid-to-particle Nusselt number and the Reynolds number is a subject of controversy. Table 5 shows the calculations. For $Re = 4$, Nelson and Galloway (*12*) would predict $Nu = 0.05$. However, Miyauchi *et al.* (*13*) propose $Nu = 8$. If

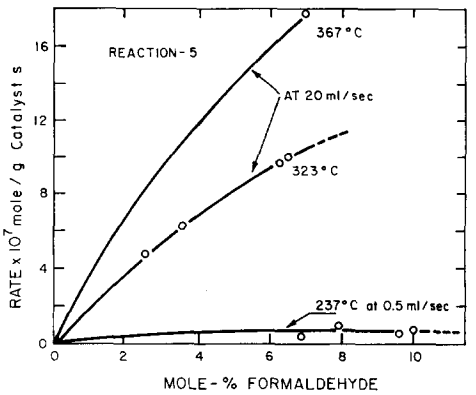


FIG. 7. Steady-state rate vs mol % formaldehyde.

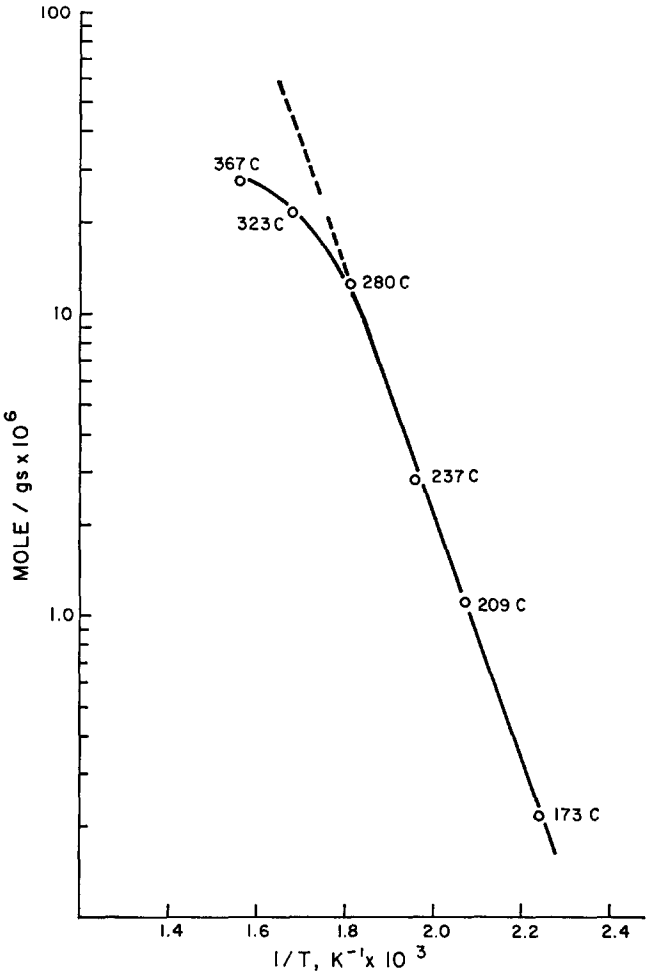


FIG. 8. Arrhenius plot of reaction 1.

$Nu = 1$ is chosen, it leads to an interphase $\Delta T$ of 15°C. Again, it is clear that heat transfer effects are beginning to become important at 280°C. Nevertheless, we consider the evidence of Fig. 8 to be more reliable than the estimations of

TABLE 3

Reaction Rate Data at Steady State

| Reference | Temperature (°C) | $r_1$ (mol/g·s) | $E_1$ (kcal/mol) |
|---|---|---|---|
| This work | 209 | $1.1 \times 10^{-6}$ | 19.5 |
| | 237 | $2.8 \times 10^{-6}$ | |
| | 280 | $12.6 \times 10^{-6}$ | |
| Bibin and Popov (*14*) | 225 | $9.8 \times 10^{-7}$ | 16–19 |
| | 270 | $5.1 \times 19^{-6}$ | |
| Jiru *et al.* (*15*) | 270 | $8.5 \times 10^{-6}$ | 13 |
| Habersberger and Jiru (*16*) | 270 | $6.6 \times 10^{-7}$ | 10.8 |
| Evmenenko and Gorokhovatskii (*6*) | | | 17.6 |

TABLE 4

Estimation of Isothermal Effectiveness Factor

| | |
|---|---|
| $T$ | = 280°C |
| $\bar{r}_v$ | = $2.71 \times 10^{-5}$ mol/cm³·s |
| $c_s$ | = $2.72 \times 10^{-7}$ mol of methanol/cm³ |
| $\theta$ | = 0.5 |
| $S_g$ | = $4.6 \times 10^4$ cm²/g |
| $\rho_p$ | = 2.15 g/cm³ |
| $r_e$ | = $1 \times 10^{-5}$ cm (100 nm) |
| $D_K$ | = 0.400 cm²/s |
| $D_{AB}$ | = 0.469 cm²/s |
| $\frac{1}{D_A}$ | $= \frac{1}{D_K} + \frac{1}{D_{AB}} = \frac{1}{0.215 \text{ cm}^2/\text{s}}$ |
| $\tau$ | = 3.0 |
| $D_{A\,\text{eff}}$ | $= D_A \theta/\tau$ = 0.0360 cm²/s |
| $R$ | = 0.042 cm |
| $\Phi_s$ | $= R^2 r_v/D_{A\,\text{eff}} c_s = 4.88 = \eta \phi^2$ |
| $\eta$ | $= \frac{3}{\phi}\left[\frac{1}{\tanh \phi} - \frac{1}{\phi}\right]$ |
| $\phi$ | = 2.60 |
| $\eta$ | = 0.720 |

TABLE 5

Estimation of Interphase Temperature Difference

| | |
|---|---|
| $\Delta T$ | $= 2(-\Delta H)\bar{r}_v R^2/3\,k\,(Nu)$ |
| $-\Delta H$ | = 36,800 cal/mol |
| $\bar{r}_v$ | = $2.71 \times 10^{-5}$ mol/cm³-s |
| $R$ | = 0.042 cm |
| $k$ | = $8 \times 10^{-5}$ cal/cm K-s |
| $Nu$ | = 1.0 |
| $\Delta T$ | = 14.7°C |

Tables 4 and 5. Of course, where both inter- and intraphase effects are important, a more involved calculation is needed for $\eta$, as described by Carberry (*10*).

For reaction 5, conversion of $CH_2O$ to CO, the activation energy found was 18.8 kcal/mol.

The results of the transient studies are given in Figs. 9–11 for a switch in feed gas composition from 4:1 $N_2$:$O_2$ carrier gas to this gas with about 16 mol % methanol at 172–173°C. Three flow rates were used as shown, corresponding to methanol conversions of 17.7% at 150 ml/min to 35% at 10 ml/min. The eventual steady states reached are those of Table 2. The input step function was obtained by quickly closing the valve in the bypass line around the methanol saturator. For even the slowest flow rate the methanol inlet concentration rose to its steady-state value in less than 1 min, a time adequately small compared to the chemical response times obtained. For this work no on-line analysis was available (e.g., a mass spectrometer) so it was necessary to do the transient runs at a temperature low enough to make the response slow enough to permit the analysis by gas chromatography. To obtain the points shown it was necessary to repeat the transients many times, with one analysis per run at a suitable time.

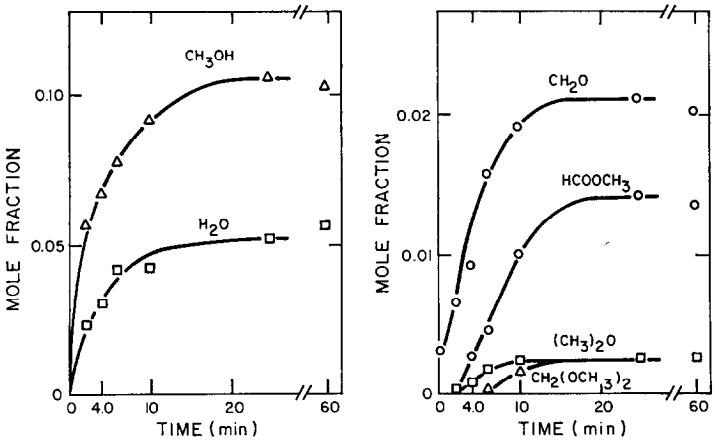


FIG. 9. Transient period: $N_2$–$O_2$ = 10 cm³/min, $T_X$ = 172°C.

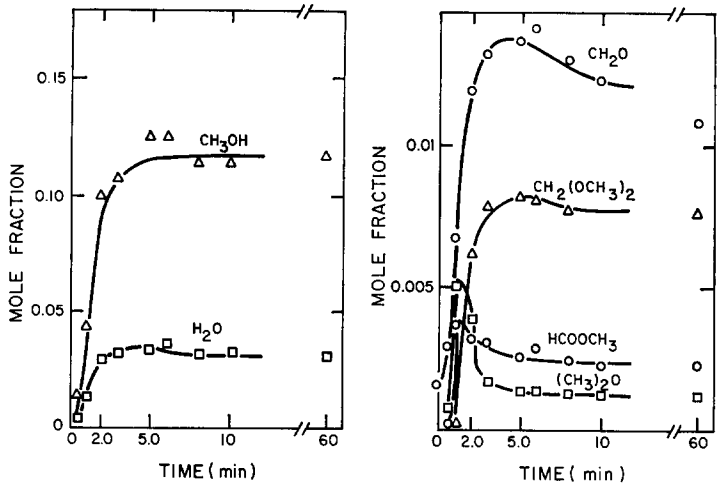


FIG. 10. Transient period: $N_2$–$O_2$ = 50 cm³/min, $T_X$ = 173°C.

As the residence time in the mixed flow reactor is reduced by increasing the flow rate, the response changes from a slow rise to an overshoot more typical of a differential reactor. This effect has been discussed and quantitatively modeled for $N_2O$ decomposition (*1*).

Complete material balances were satisfied for all the steady-state conditions and served as a check on the chromatograph response factors and the general precision of the experiments (*8*).

## DISCUSSION

The results of the steady-state experiments at temperatures above 209°C confirm the features observed by others and already mentioned: The reaction is approximately first order in methanol at low concentration followed by saturation of the surface and shift of the rate-determining step to desorption, especially at low temperature. The inhibition by products was also confirmed.

At about 170°C the high residence time

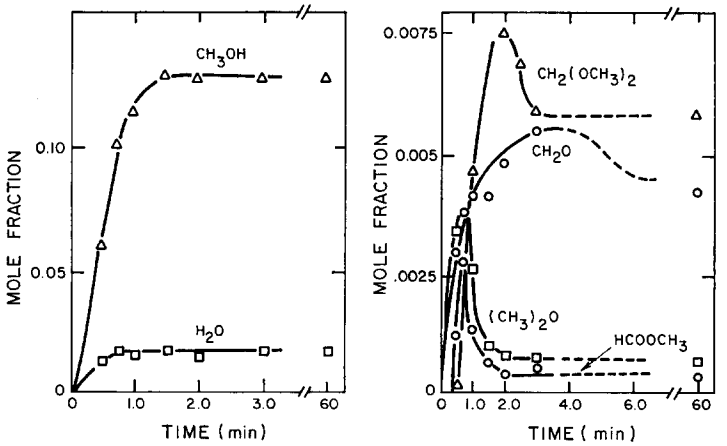


FIG. 11. Transient period: $N_2$–$O_2$ = 150 cm³/min, $T_X$ = 172°C.

of surface intermediates apparently leads to the observed byproducts. On the basis of the information now available, the following explanation is suggested. The formation of $(CH_3)_2O$ (rate $r_2$) needs no oxidative dehydrogenation and leaves the catalyst in its original oxidized state. Its formation is more probable (compared to other products) at high conversion when less oxygen is available on the surface than at low conversion. These ideas are confirmed by Figs. 9–11, although $r_2$ decreases with conversion as shown in Table 2. The probable sequence is:

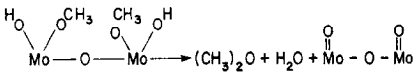

(8)

Further residence time on the oxygen-rich surface leads to dehydrogenation.

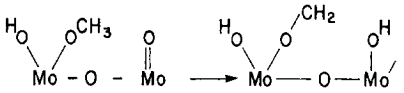

(9)

Formaldehyde may now desorb, and the surface can be reoxidized, forming water. However, adsorbed formaldehyde may react with more methanol

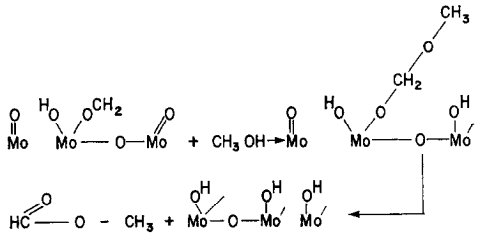

(10)

Thus, methyl formate is formed and the surface can be regenerated by oxygen with the formation of water. Methyl formate is more abundant at high conversion than low because at low conversion (high methanol partial pressure) the adsorbed oxygenated species reacts still further with methanol to give methylal.

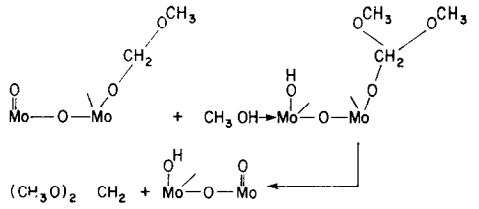

(11)

The transient in Figs. 9 and 10 show that $HCOOCH_3$ and $(CH_3)_2O$ are intermediates that are formed at first from adjacent $OCH_3$ groups and their initial products of oxidation. The adsorbed form of methyl formate reacts with gaseous methanol to form methylal, which reaches its peak later. Methylal and formaldehyde also have overshoots because the surface oxygen concentration eventually falls, to be at least partly replaced by OH groups.

At higher temperatures formaldehyde must desorb more readily, and $CH_3O$ must dehydrogenate more readily, to explain the improved selectivity for $CH_2O$ observed at higher temperatures. The discussion here is qualitative, since a detailed computer model would need to be very complicated. Future transient studies will be continued at higher temperatures with an on-line mass spectrometer; under these conditions the reaction network should be more tractable. However, the present results just below the usual reacting temperature help in understanding the surface chemistry, in particular the important part played by the methoxyl groups.

## NOMENCLATURE

| | |
|---|---|
| $i$ | = $i$th reaction in a network |
| $j$ | = $j$th chemical species |
| $r_i$ | = rate of $i$th reaction, mol/s-g |
| $y_j$ | = mole fraction of $j$th component in mixed flow reactor |
| $y_{fj}$ | = mole fraction of $j$th component in reactor feed stream |
| $F_0$ | = total feed rate, mol/s |
| $F_p$ | = total product rate, mol/s |
| $W$ | = catalyst weight, g |

$\alpha_{ij}$ = stoichiometric coefficient

$\bar{\alpha}_i = \sum_{j=1}^{N} \alpha_{ij}$

$T$ = gas temperature, °C

$\bar{r}_v$ = observed reaction rate, mol/cm³-s

$c_s$ = surface concentration of methanol, mol/cm³

$\theta$ = catalyst porosity

$S_g$ = surface area, cm²/g

$\rho_p$ = catalyst pellet density, g/cm³

$r_e$ = mean pore diameter, cm

$D_K$ = Knudsen diffusivity, cm²/s

$D_{AB}$ = diffusivity of methanol through air, cm²/s

$\tau$ = tortuosity

$R$ = pellet radius, cm

$\phi$ = Thiele modulus

$\eta$ = effectiveness factor

$-\Delta H$ = heat of reaction, cal/mol

$k$ = thermal conductivity of air, cal/cm-s-°C

$Nu$ = Nusselt number, $2Rh/k$

$h$ = heat transfer coefficient, cal/cm²-°C

ACKNOWLEDGMENT

The financial support of NSF Grant ENG 72-04165 is gratefully acknowledged.

REFERENCES

1. Bennett, C. O., *Catal. Rev. Sci. Eng.* **13**(2), 121 (1976).
2. Pernicone, N., Lazzerin, F., Liberti, G., and Lanzavecchia, G., *J. Catal.* **14**, 293 (1969).
3. Jiru, P., Wichterlová, B., Kriván ek, M., and Novaková, A., *J. Catal.* **11**, 182 (1968).
4. Mars, P., and van Krevelen, D. W., *Chem. Eng. Sci.* (special supplement) **3**, 41 (1954).
5. Jiru, P., Wichterlová, B., and Tichy, J., *in* "Proceedings 3rd International Congress on Catalysis." Amsterdam, 1964, p. 199.
6. Evmenenko, N. P., and Gorokhovatskii, Ya. B., *Kinet. Katal.* **10**, 1071 (1969).
7. Novakova, J., Jiru, P., and Zavadil, V., *J. Catal.* **21**, 143 (1971).
8. Edwards, James, M.S. Thesis, University of Connecticut, 1976.
9. Aruanno, Jorge, and Wanke, Sieghard, *Canad. J. Chem. Eng.* **53**, 301 (1975).
10. Carberry, J. J., "Chemical and Catalytic Reaction Engineering." McGraw-Hill, New York, 1976.
11. Satterfield, C. N., "Mass Transfer in Heterogeneous Catalysis." MIT Press, Cambridge, Massachusetts, 1970.
12. Nelson, P. A., and Galloway, T. R., *Chem. Eng. Sci.* **30**, 1 (1975).
13. Miyauchi, T., Kataoka, H., and Kikuchi, T., *Chem. Eng. Sci.* **31**, 9 (1976).
14. Bibin, U. N., and Popov, B. I., *Kinet. Katal.* **10**, 1091 (1969).
15. Jiru, P., Tichy, J., and Wichterlová, B., *Coll. Czech. Chem. Commun.* **31**, 674 (1966).
16. Habersberger, K., and Jiru, P., *Coll. Czech. Chem. Commun.* **37**, 535 (1972).